Validation of Special Sensor Microwave Imager Monthly-Mean Wind Speed From July 1987 to December 1989

David Halpern

Earth and Space Sciences Division

Jet Propulsion Laboratory

California Institute of Technology

Pasadena, CA 91109

(telephone: 818-354-5327)

(fax: 818-393-6720)

(telemail: D.HALPERN/omnet)

ABSTRACT

Since July 1987 the Remote Sensing Systems, Santa Rosa, California, routinely computes from first principles the wind speed from Special Sensor Microwave Imager (SSM/I) measurements of the intensity of microwave radiation emitted at the ocean surface. The accuracy of monthly-mean SSM/I wind speeds is determined by comparisons with moored-buoy wind measurements, which were recorded by four different institutions at 44 sites in the Atlantic and Pacific Oceans during July 1987 to December 1989. All results for 1988 were virtually identical with 1989. The range of monthly mean moored-buoy wind speeds was 2 - 10 m s^{-1}. During 1987, the equatorial matchups were not equivalent with 1988 and 1989, and the cause remains unknown. The root-mean-square (rms) difference of 697 monthly-mean matchups of the composite 1988 and 1989 data set was 1.2 m s^{-1}. The rms differences were smaller in the equatorial zone and higher in middle latitudes, in accord with the monthly standard deviation. At middle latitudes the time series of rms differences displayed an annual cycle. In the equatorial zone the agreement between SSM/I and *in situ* data was better in regions with a lesser amount of clouds, and *vice versa*. For SSM/I monthly standard deviations of 1 - 2, 2 - 3, and 3 - 4 m s^{-1}, the average absolute values of the monthly-mean difference between SSM/I and moored-buoy wind speeds were 0.6, 0.9, and 1.4 m s^{-1}, respectively.

I. INTRODUCTION

The Intergovernmental Panel on Climate Change [1] stated that ocean-atmosphere interactions are a high-priority subject for expansion of research in order to reduce the uncertainties associated with predictions of global warming. Long time series of monthly-mean distributions of geophysical variables, which cover the globe or a large-scale region like an entire ocean basin, are becoming *de rigueur* for studies of the seasonal cycle and interannual climate variations. The present lack of adequate oceanographic data to support global ocean and coupled ocean-atmosphere general circulation models dictates a need to improve our ability to make use of satellite data.

The surface wind speed, S, is an important variable in ocean-atmosphere interactions: air-sea

latent and sensible heat fluxes and air-sea transfer rate of carbon dioxide are each proportional to S, momentum flux is proportional to S^2, and the rate of working of the wind stress on the surface layer of the ocean is related to S^3. However, because of numerous difficulties, the *in situ* surface wind field over the ocean has been extremely undersampled. Satellites provide frequent coverage of global measurements; yet, satellite-borne instrumentation does not directly measure near-surface wind speed. Electromagnetic radiation measurements recorded on the spacecraft are related to the 10-m height wind speed.

A Hughes Aircraft 7-channel, 4-frequency, linearly-polarized, passive microwave radiometer, which is called the Special Sensor Microwave Imager (SSM/I), was launched on 19 June 1987 on the U.S. Air Force Defense Meteorological Satellite Program (DMSP) spacecraft F8. The DMSP SSM/I measurement program is expected to continue for about 10 years. A second and third SSM/I were launched on DMSP spacecrafts F10 and F11 on 1 December 1990 and 28 November 1991, respectively. Coverage of SSM/I 10-m height wind speeds over the global ocean is nearly complete every 3 days [2]. The global distribution of the approximate 2 wind speed observations per day per 1/3° x 1/3° area [2] represents nearly 2000 times more data than are available from the volunteer observing ship network. A unique feature of the global distribution of SSM/I 10-m height wind speeds is its minimal aliasing.

Intensity of microwave radiation emitted at the ocean surface is affected by roughness of the sea surface, which is correlated with the 10-m height wind speed. Several algorithms [3, 4, 5, 6] exist to convert radiances measured at the DMSP spacecraft into 10-m height wind speeds. The Remote Sensing Systems (RSS), Santa Rosa, California, uses the Wentz procedure [3, 7] to routinely process SSM/I data into 10-m height wind speed over the ocean. The RSS-derived SSM/I wind speeds are available from the NASA Ocean Data System [8]. The accuracy of monthly-mean RSS-created SSM/I 10-m height wind speeds, which is the subject of this report, is determined by comparisons with moored-buoy wind measurements at numerous sites in the Pacific and Atlantic Oceans.

II. MEASUREMENT TECHNIQUES

A. SSM/I Wind Speed

The RSS algorithm computes *ab initio* the wind speed at 19.5-m height, $S_{19.5m}$ in m s^{-1}, with SSM/I measurements from only the 37-GHz channels. Two equations are solved [7, 9]:

$$T_{Bv} = F_v(S_{19.5m},\tau) \quad (1)$$

$$T_{Bh} = F_h(S_{19.5m},\tau) \quad (2)$$

where T_{Bv} and T_{Bh} are the 37-GHz vertically and horizontally polarized brightness temperature observations, respectively, and τ is the total one-way atmospheric transmittance along the viewing path of the radiometer. F_v indicates that T_{Bv} is a function of $S_{19.5m}$ and τ; similarly for F_h. In the absence of rain, the atmosphere is relatively transparent at 37 GHz with τ equal to 0.75 to 0.95, depending on humidity. The $F_v(S_{19.5m},\tau)$ and $F_h(S_{19.5m},\tau)$ are explicitly described in terms of $S_{19.5m}$, τ, air and sea surface temperatures, and the incidence angle. The $S_{19.5m}$ is determined by Newton's iteration method, and convergence is defined when the difference between iterations becomes less than 0.05 m s^{-1}. If convergence is not reached after 10 iterations, which was arbitrarily chosen, then the 37-GHz brightness temperatures were not used. When $S_{19.5m}$ was negative, which occurred about 1% of the time, it was deleted from further processing. The SSM/I 10-m height wind speed is equal to $0.943S_{19.5m}$ [3].

The RSS determines the liquid water content in the atmosphere from SSM/I measurements concurrently with estimates of the 10-m height wind speed. If the total liquid water content throughout the atmosphere is greater than 0.25 kg m^{-2}, then the wind-speed algorithm is considered invalid because there would be too much radiative scattering from water droplets. Brightness temperatures measured within about 100 km of land are not used to estimate wind speed because the emissivity of land is very different from that of water. For the same reason, the wind speed within 200 km of the ice edge, which is determined concurrently by RSS from SSM/I measurements, are not used.

The SSM/I was turned off from 2 December 1987 to 12 January 1988 to avoid possible damage of the instrument by increased heating of the bearing and power transfer assembly [10].

During December 1988 and December 1989, the DMSP spacecraft solar arrays were repositioned so that the SSM/I was not again turned off.

B. Moored-Buoy Wind Speed

Moored-buoy wind measurements from four institutions are used (Figure 1), with about 45% from the National Oceanic and Atmospheric Administration (NOAA) National Data Buoy Center (NDBC) and approximately 50% from the NOAA Pacific Marine Environmental Laboratory (PMEL). Not all buoy sites yielded wind observations throughout the validation period.

The NDBC moored-buoy wind measurements were made in the northwest Atlantic, throughout the North Pacific, and a site in the southeast Pacific. A propeller-vane anemometer recorded once every hour an 8-min average of the wind speed and a single direction with accuracies of $\pm$ 1.0 m s^{-1} or 10%, whichever is greater, and $\pm$ 10° [11]. Pre-deployment anemometer calibrations yielded errors of 0.25 m s^{-1} and 2.5°. The height of the anemometer varied between 4.9 and 13.8 m, with most anemometers at about 5 m. The data are telemetered hourly via the Geostationary Operational Environmental Satellite spacecraft to a NOAA facility at Wallops Island, Virginia, and then transferred to NDBC, where data quality are examined. The NDBC hourly wind speed (in knots) and direction data are used herein. The hourly Cartesian wind components (in m s^{-1}) were computed and, thence, daily vector-averaged scalar speeds were computed from the 24-h vector-averaged east-west and north-south components.

The PMEL moored-buoy wind measurements were made at 3.8-m height in the tropical Pacific Ocean. At most locations, a propellor-vane anemometer sampled wind speed and direction at 2 Hz and recorded 1-h or 2-h vector-averaged east-west and north-south components [12]. Pre- and post-deployment wind-tunnel tests indicated that propellor-vane measurements are accurate to within 0.2 m s^{-1} in speed and 5° root-mean-square (rms) in direction [13]. The data are telemetered to PMEL in Seattle via the ARGOS navigational system on NOAA spacecraft. Five unique data transmissions are normally received each day, and are used to compute daily vector-averaged Cartesian components. Daily vector-averaged scalar speeds were computed from the daily vector-

mean east-west and north-south components. Three of the PMEL moorings contained a 3-cup anemometer and vane, which internally measured 15-min vector-averaged wind components, and daily vector-averaged scalar speeds are used herein. Moored wind data recorded by propellor-vane and cup-vane anemometers were equivalent to 0.1 m s^{-1} [13], and are considered interchangeable.

The Woods Hole Oceanographic Institution (WHOI) moored-buoy wind measurements were made at 3-m height at a single location in the northwest Atlantic. A propellor-vane wind recorder measured 15-min vector-averaged east-west and north-south components, and internally stored the data. These data were used herein. Daily vector-averaged scalar speeds were computed. Pre- and post-calibration of the wind propellor indicated a calibration shift of less than 1% [14].

The Japan Meteorological Agency (JMA) maintains four deep-ocean moored buoys in the northwest Pacific. Wind speed and direction at 7.5-m height are recorded continuously for 10 min every 3 hours with a 3-cup anemometer and wind vane, and the 10-min average wind speed and direction are transmitted to JMA in Tokyo. The accuracies of the wind speed and direction are about ± 1.5 m s^{-1} and 5°, respectively [H. Masuko, personal communication, 1992]. The data from one of the four moored buoys are used herein; the 3 other moored buoys were located close to Japan. The 3-hourly wind speeds and directions were converted to Cartesian components, which were then averaged in non-overlapping groups of eight samples. Daily vector-averaged wind speeds were computed.

Mooring motion influences wind measurements from surface-following buoys which move horizontally and vertically to follow the contour of the sea surface. In a comparison of wind speed data recorded from a toroidal buoy, which is the surface float for the PMEL moorings and typical of surface-following buoys, and a vertically stable spar buoy, which were separated by 9 km near 0°, 110°W, the toroid wind speeds were 3% higher than corresponding spar speeds for 15-min averaged data and 2% higher for 8-hour averages (correlation coefficient = 0.98) [15]. No adjustments of the daily-averaged wind speeds were made for mooring motion, although the effects of mooring motion in extra-tropical latitudes may be larger because of the higher wind and wave conditions.

III. METHODS

A. SSM/I Wind Speed

The SSM/I wind-speed values occur in nonoverlapping areas of 25 km x 25 km, which are arrayed across the 1394-km swath width. Geographical coordinates correspond to the center of each 25-km x 25-km region. All speeds located within nonoverlapping 1/3° x 1/3° squares were arithmetically averaged each day. The 1/3° x 1/3° area was chosen to correspond to the horizontal grid of an ocean general circulation model used to simulate wind-driven upper-ocean currents in the tropical Pacific, and because it is the pixel size of a number of satellite-derived data products published in a series of atlases [2, 9]. Most 1/3° x 1/3° areas contained about 2 wind values per day. Areas with excessive amounts of atmospheric moisture, such as the Intertropical Convergence Zone (ITCZ) and the South Pacific convergence zone, contained about 1 wind speed measurement per day [9, 2]. Aliasing of the diurnal-period oscillation probably did not influence longer time scales because of the smallness of the rms amplitude of the diurnal-period surface wind, which was 0.3 m s^{-1} along the Pacific equator [16] and 0.4 m s^{-1} within the Pacific ITCZ [17]. The observed diurnal-cycle amplitudes were similar to the diurnal wind vectors produced by the European Center for Medium-Range Weather Forecasts (ECMWF) forecast-analysis system [18], which indicated similar values would be expected at all our buoy sites, except at the 18°S, 85°W buoy where the magnitude was two times larger.

At each buoy site a daily-averaged 2/3° x 2/3° wind-speed value was computed by arithmetically averaging the daily 1/3° x 1/3° speeds located within a 2 x 2 matrix centered at the nominal site of the moored buoy. The nominal location of each buoy was defined as the nearest integer latitude and longitude. For a time scale of 1 day, moored buoy wind measurements separated by 115 km in the central and eastern equatorial Pacific were coherent with 95% statistical significance and with zero phase difference [16]; within the ITCZ the horizontal coherence was lower, as expected, and not 95% statistically significant [17]. During July 1987 to December 1989, approximately 65% of the daily-averaged 2/3° x 2/3° wind-speed values were computed with a daily speed in each of the four 1/3° x 1/3° elements of the 2 x 2 matrix. Approximately 72% of

the 2/3° x 2/3° values were the average of three or four daily 1/3° x 1/3° elements. No daily 1/3° x 1/3° values occurred within a 2 x 2 matrix about 18% of the time.

A monthly-mean 2/3° x 2/3° wind speed, $S_{SSM/I}$, was calculated if the number of daily-averaged 2/3° x 2/3° wind-speed values was greater than 19 within a calendar month. Months with less than 20 daily-averaged 2/3° x 2/3° wind speeds within a calendar month were deleted from analysis. The choice of 20 days as the lower limit to form monthly-mean wind speeds was not entirely arbitrary [19].

B. Moored-Buoy Wind Speed

Moored-buoy wind measurements were referenced to 10-m height, assuming a logarithmic wind profile, von Kármán's constant of 0.4, neutral stratification, and a wind-speed dependent drag coefficient [20]. For example, the PMEL 3.8-m height wind speed, $S_{3.8m}$, referenced to 10-m height is equal to $1.089S_{3.8m}$. A monthly-mean moored-buoy 10-m height wind speed, S_{BUOY}, was computed if the number of daily-averaged wind-speed values was greater than 19 within a calendar month.

C. Statistical Significance Tests

The statistical significance between two mean values, X_1 and X_2, which were each computed for a small number of values, is determined from the distribution of Student's t [21],

$$t = (X_1 - X_2) / (((\Sigma x_1^2 + \Sigma x_2^2)/(N_1 + N_2 - 2))((N_1 + N_2)/N_1N_2))^{1/2}) \qquad (3)$$

where N_1 and N_2 are number of data values in the estimation of X_1 and X_2, respectively, and x_1 and x_2 are the deviations of the individual values from their respective means. For X_1 and X_2 to be considered different with some degree of confidence, t must be greater than the appropriate value listed in Fisher's Table of t. For 95% statistical significance, which is the confidence level used throughout the paper, the t values corresponding to degrees of freedom of 10, 20, and 30 are approximately 2.22, 2.09, and 2.04, respectively. The number of degrees of freedom is defined by $N_1 + N_2 - 2$. For an infinite number of degrees of freedom the t value is 1.96.

The statistical significance between two correlation coefficients, r_1 and r_2, which were each computed for a moderately large (> 10) number of values, is computed with Fisher's z-transformation. For each measured correlation coefficient, r, the corresponding z is [22]

$$z = (1/2)\ \ln((1+r)/(1-r)). \qquad (4)$$

The significance of a difference between r_1 and r_2 is given by w, which is defined by

$$[(|z_1 - z_2|) / ((\sqrt{2})\ ((1/(N_1 - 3)) + (1/(N_2 - 3)))^{1/2})] \qquad (5)$$

where N_1 and N_2 are number of data values in the measurement of r_1 and r_2, respectively. For 95% statistical significance that r_1 and r_2 are different, w must be greater than 1.96.

IV. INTERCOMPARISONS AT PMEL AND WHOI MOORED-BUOY SITES

The PMEL and WHOI wind-recording systems were very similar. Of the 22 maximum number of sites, 21 were PMEL buoys.

A. Root-Mean-Square Differences

Each month the rms difference was computed between all pairs of $S_{SSM/I}$ and S_{BUOY} values (Figure 2A). The number of buoy sites with coincident pairs of $S_{SSM/I}$ and S_{BUOY} increased steadily from two at the time of the launch of DMSP F8 to twenty about 2 years later (Figure 2B). The maximum monthly rms difference, which occurred in October 1987, was 2.4 m s^{-1}, and the only other occasion when the monthly rms difference was greater than 2 m s^{-1} occurred in September 1987. The July - November 1987 mean rms difference was 2.0 m s^{-1}, which was more than double the annual-mean rms difference during 1988 or 1989. The difference between 1987 and either 1988 or 1989 mean values of rms difference was 95% statistically significant. The annual-mean 1988 and 1989 rms differences were the same with 95% confidence.

B. Orthogonal Regressions

An orthogonal regression line, which minimizes the perpendicular distance from the regression line, was computed at each buoy site when there were at least 12 coincident pairs of

S_{BUOY} and $S_{SSM/I}$ values during 1988 and 1989 (Figure 3). The rms differences between $S_{SSM/I}$ and S_{BUOY} and between standard deviations (not shown) during 1987 were large and 95% statistically different compared to 1988 and 1989. Another representation of a substantial difference between $S_{SSM/I}$ and S_{BUOY} matchups during 1987 compared to subsequent years is indicated by the correlation coefficient calculated between coincident pairs. During 1987 the correlation coefficient was 0.63, which was 20% smaller than in 1988 or 1989 and which was 95% statistically different than the correlation coefficients during 1988 and 1989. The difference between the 1988 and 1989 correlation coefficients was not significant with 95% confidence.

The PMEL data for 1987 were not used in further analysis because the 1987 average difference was substantially larger than that during 1988 or 1989 (§IV.A) and because the 1987 average correlation coefficient was significantly smaller than that during 1988 or 1989. The statistical results obtained during 1987 might have been influenced by the relatively small number of test sites (Figure 1B). The average monthly number of test sites in 1987, 1988, and 1989 were 7, 12, and 17, respectively. The cause of the poor matchups between moored-buoy and SSM/I wind speeds during 1987 remains unknown.

At 2°N, 140°W the 1988-89 regression line was anomalously different than the others (Figure 3) because the correlation coefficient was not statistically significant at the 95% confidence level. The 1988 correlation coefficient was not significant; however, the 1989 data were 95% statistically correlated. The 2°N, 140°W data set was deleted from further analysis.

Regression analyses for the 117 matchups during 1988 and 178 coincident pairs during 1989 were very similar (Figure 4). Characteristics of the combined 295 pairs of monthly-mean S_{BUOY} and $S_{SSM/I}$ during 1988 and 1989 were: (i) mean $S_{SSM/I}$ was 0.2 m s^{-1} smaller than S_{BUOY}; (ii) rms difference was 0.9 m s^{-1}; (iii) correlation coefficient between $S_{SSM/I}$ and S_{BUOY} data was 0.82, indicating that more than half of the variance caused by month-to-month fluctuations of each data set was linearly related; (iv) the orthogonal regression line was $S_{SSM/I}$ (m s^{-1}) = 0.13 + 0.95 S_{BUOY} (m s^{-1}); (v) difference between $S_{SSM/I}$ predicted from S_{BUOY} increased with wind speed, becoming 4% at 10 m s^{-1}.

C. Geographical Features

The space-time structure of the surface wind field within about 5° of the equator is important because wind forcing of upper-ocean thermal and flow fields is associated with the generation, maintenance, and dissipation of El Niño episodes [23]. During 1989 there were moored buoys along the equator at 165°E, 169°W, 140°W, 124°W, 110°W, which produced 54 $S_{SSM/I}$ and S_{BUOY} pairs. The matchups were strongly correlated, with a correlation coefficient of 0.89, and the rms difference at 0.72 m s^{-1} was 20% smaller than the composite value.

During 1989 several moored-buoy sites also existed simultaneously along two longitudes: 110°W (5°S, 2°S, 0°, 2°N, 5°N) and 165°E (5°S, 2°S, 0°, 2°N, 5°N, 8°N). Although the rms differences between $S_{SSM/I}$ and S_{BUOY} matchups were approximately 1.0 m s^{-1} along 110°W and 165°E, the correlation coefficients were 0.89 and 0.68 along 110°W and 165°E, respectively. The difference between the two correlation coefficients was significant at the 95% level. The lower degree of linearity between $S_{SSM/I}$ and S_{BUOY} along 165°E compared to 110°W was probably caused by the degradation of the SSM/I wind speed retrieval because of increased atmospheric liquid water content along 165°E. The 1989-annual average outgoing longwave radiation (OLR), which represents the amount of cloud, from 5°S to 5°N along 165°E and 110°W were 245 W m^{-2} and 265 W m^{-2}, respectively [24]. The higher the OLR, the dryer the air, *e. g.*, over the Sahara Desert the OLR is 290 - 300 W m^{-2}. The OLR is routinely used in atmospheric sciences as an indicator of clouds, which is analogous to total liquid content in the atmosphere because virtually all the atmospheric liquid water resides in the troposphere. The RSS-derived total liquid water content from SSM/I measurements was not used because it had been used in the estimation of wind speeds and, therefore, it was not independent of the RSS-derived wind speeds.

V. INTERCOMPARISONS AT NDBC AND JMA MOORED-BUOY SITES

The NDBC and JMA wind-recording systems were very similar. Of the 21 maximum number of sites, 20 were NDBC buoys.

A. Root-Mean-Square Differences

Each month the rms difference was computed between all pairs of $S_{SSM/I}$ and S_{BUOY} values. The maximum rms difference between $S_{SSM/I}$ and S_{BUOY} values, which occurred in April 1988, was slightly less than 2 m s^{-1}. The rms differences were lowest during June, July, August and September in 1987, 1988, and 1989 (Figure 5A); the average rms difference was 0.8 m s^{-1}. Large rms differences occurred during northern hemisphere winter months; the average rms difference during December, January, February and March was 1.6 m s^{-1}. The range of the annual cycle was significant.

The standard deviation of daily values of the monthly moored-buoy wind speeds was computed whenever there was a $S_{SSM/I}$ and S_{BUOY} matchup. The time series of the average monthly-mean standard deviations (Figure 5B) displayed an annual variation. The June-to-September average value was 2.3 m s^{-1}, which was about 0.6 m s^{-1} smaller than the average December-to-March value. The range of the annual cycle of the average monthly-mean standard deviations was 95% statistically significant.

The July-to-November magnitudes and pattern of the rms difference time-series in 1987 were repeated in 1988 and again in 1989 (Figure 5A), in marked contrast to the situation found in the tropical Pacific (Figure 2A) where the features for 1987 were different than in 1988 and 1989. In 1987 there were considerably more NDBC intercomparison sites (Figure 5C) than PMEL sites (Figure 2B).

B. Orthogonal Regressions

An orthogonal regression line was computed at each buoy site where at least 12 coincident pairs of S_{BUOY} and $S_{SSM/I}$ occurred during 1987-89. The correlation coefficient at each intercomparison site was statistically significant at the 95% level; the ensemble-average correlation coefficient was 0.88.

Regression analyses for 1987, 1988, and 1989 when there were 69, 143, and 132 matchups, respectively, are shown in Figure 6. The annual regression lines, correlation coefficients, and rms

differences were virtually identical. Characteristics of the 344 pairs of $S_{SSM/I}$ and S_{BUOY} from July 1987 to December 1989 were: (i) mean $S_{SSM/I}$ was 0.8 m s^{-1} larger than S_{BUOY}; (ii) rms difference was 1.3 m s^{-1}; (iii) correlation coefficient between $S_{SSM/I}$ and S_{BUOY} data was 0.85, indicating that more than half of the variance caused by month-to-month fluctuations of each data set was linearly related; (iv) the orthogonal regression line was $S_{SSM/I}$ (m s^{-1}) = -2.3 + 1.5 S_{BUOY} (m s^{-1}) for wind speeds between 2.5 and 12 m s^{-1}; (v) difference between $S_{SSM/I}$ predicted from S_{BUOY} increased with wind speed, becoming 27% at 10 m s^{-1}. That the computed $S_{SSM/I}$ would be ≤ 0 m s^{-1}, which is nonsense, for $S_{BUOY} \leq 1.5$ m s^{-1} means that the regression line was not appropriate for $S_{BUOY} \leq 1.5$ m s^{-1}. The form of the regression curve at wind speeds less than 2.5 m s^{-1} is unknown.

VI. INTERCOMPARISONS AT COMPOSITE MOORED-BUOY TEST SITES

An orthogonal regression analysis was made of all PMEL (omitting 2°N, 140°W), JMA, NDBC, and WHOI 1988 and 1989 S_{BUOY} and $S_{SSM/I}$ matchups. Characteristics of the 697 pairs were: (i) mean $S_{SSM/I}$ was 0.25 m s^{-1} larger than S_{BUOY}; (ii) rms difference was 1.2 m s^{-1}; (iii) correlation coefficient between $S_{SSM/I}$ and S_{BUOY} data was 0.77, indicating that more than half of the variance caused by month-to-month fluctuations of each data set was linearly related; (iv) the orthogonal regression line was $S_{SSM/I}$ (m s^{-1}) = -1.7 + 1.3 S_{BUOY} (m s^{-1}) for wind speeds between 2 and 12 m s^{-1}; (v) difference between $S_{SSM/I}$ predicted from S_{BUOY} increased with wind speed, becoming 13% at 10 m s^{-1}.

The entire group of $S_{SSM/I}$ and S_{BUOY} matchups (except at 2°N, 140°W) for 1988 and 1989 was partitioned into 10°-latitude bands, *e. g.*, from 5°S - 5°N and 45°N - 55°N. The average correlation coefficient and rms difference between $S_{SSM/I}$ and S_{BUOY} matchups, and the average standard deviation of the moored-buoy wind speeds were computed for each 10° band for 1988 and 1989. The smallest number of matchups per 10° band was 10; the maximum was 126. Results for 1988 and 1989 were very similar. The 1988-89 correlation coefficients showed no

distinct trend with latitude. The 1988-89 values of the rms differences and average standard deviations were different north and south of 25°N. From 25°S - 25°N, the rms differences and average standard deviations were both approximately constant at about 0.8 m s^{-1} and 1.6 m s^{-1}, respectively. Northward of 25°N, the rms differences increased continuously with a 25 - 65°N average value of 1.5 m s^{-1} and the average standard deviations were uniform at about 2.8 m s^{-1}. The large latitudinal variations of the rms differences and of the monthly standard deviations occurring at about 25°N were both statistically significant at the 95% level.

The previous suggestion of a latitudinal dependence of the accuracy of SSM/I wind retrievals, while appealing [25], is misleading because the RSS determination of $S_{SSM/I}$ is independent of latitude. The natural variability of the surface wind, which is strongly dependent upon season and thereby also upon latitude [2], reduces the agreement between $S_{SSM/I}$ and S_{BUOY}. The $S_{SSM/I}$ - S_{BUOY} difference was related to the monthly standard deviation of $S_{SSM/I}$, $(S_{SSM/I})_{std\ dev}$. The average absolute value of the $S_{SSM/I}$ - S_{BUOY} difference, $|S_{SSM/I} - S_{BUOY}|$, was computed for each 0.25 m s^{-1} interval of $(S_{SSM/I})_{std\ dev}$ (Figure 7): correlation coefficient was 0.86; rms difference was 1.6 m s^{-1}; regression line was $|S_{SSM/I} - S_{BUOY}|$ (m s^{-1}) = 0.25 + 0.31 S_{BUOY} (m s^{-1}). An alternate interpretation of the trend indicated by the scatter plot is a uniform $|S_{SSM/I} - S_{BUOY}|$ value of 0.7 m s^{-1} for 0.75 m $s^{-1} \leq (S_{SSM/I})_{std\ dev} \leq 2.5$ m s^{-1}, and a 1.0 to 1.75 m s^{-1} linear trend of $|S_{SSM/I} - S_{BUOY}|$ for 2.5 m $s^{-1} \leq (S_{SSM/I})_{std\ dev} \leq 4.0$ m s^{-1}. The average $|S_{SSM/I} - S_{BUOY}|$ values were associated with large uncertainties, which are represented in Figure 7 with vertical lines, and analyses of matchups for 1990 and 1991 will improve the estimates of the uncertainty.

VII. SUMMARY AND CONCLUSIONS

Algorithms relating radiation measurements at a satellite to surface wind speed are complex, and several different SSM/I algorithms exist. This situation is very different from that of *in situ* wind-measuring instrumentation, which is calibrated in a wind tunnel which itself is calibrated against a reference traceable to a single standard. The RSS-created wind speeds were routinely

produced, continue to be routinely produced, and are freely available. The S_{BUOY} and $S_{SSM/I}$ were independent measures of the 10-m height monthly-mean wind speed. The range of monthly mean moored-buoy wind speeds was 2 - 10 m s^{-1}, which did not adequately encompass the environment poleward of about 45° where higher monthly mean wind speeds occur during winter season [2, 9].

The agreement between $S_{SSM/I}$ and PMEL S_{BUOY} data was not satisfactory during 1987 compared with 1988 and 1989. The 1987 rms differences between PMEL S_{BUOY} and $S_{SSM/I}$ were significantly larger than in 1988 and 1989. The 1987 correlation coefficient computed between $S_{SSM/I}$ and PMEL S_{BUOY} matchups was substantially smaller than the corresponding correlation coefficients for 1988 and 1989. Furthermore, the 1987 differences between PMEL S_{BUOY} and $S_{SSM/I}$ increased linearly with wind speed; no such relationship was found during 1988 and 1989. In contrast, the $S_{SSM/I}$ and NDBC S_{BUOY} data were in similar agreement in 1987, 1988 and 1989. The cause of the significant differences between PMEL S_{BUOY} and $S_{SSM/I}$ during 1987 compared to 1988 and 1989 is unknown. The SSM/I radiometer functioned according to engineering specifications during the July 1987 to December 1989 period [10], except for the December 1987 - January 1988 interval when the instrument was turned off. The RSS data processing procedure was unchanged during the July 1987 to December 1989 period [9, 2]. Why the results of the comparison between $S_{SSM/I}$ and PMEL S_{BUOY} data were different in 1987 compared with 1988 and 1989 remains an enigma, and requires further investigation.

The monthly standard deviation of $S_{SSM/I}$, which is an easily calculable quantity [9, 2], provides an estimate of the accuracy of $S_{SSM/I}$. For monthly standard deviations of 1 - 2 m s^{-1}, which cover approximately 27% of the SSM/I coverage of the global ocean, the average $|S_{SSM/I} - S_{BUOY}|$ was 0.6 m s^{-1}. For monthly standard deviations of 2 - 3 and 3 - 4 m s^{-1}, which cover approximately 40 and 28% of the global ocean, respectively, the average $|S_{SSM/I} - S_{BUOY}|$ values were 0.9 and 1.4 m s^{-1}, respectively.

The SSM/I wind measurements were more accurate than wind speed measurements recorded routinely on ships, where uncertainties of ship winds were 3 - 4 m s^{-1} in middle latitudes [27]. The SSM/I represents a great advancement of global wind-measuring technology because of its

high spatial and temporal resolutions throughout the global ocean and because of its improved accuracy compared to ship reports which, before the introduction of satellite measurements, were virtually the entire source of surface wind data.

Results are encouraging to utilize $S_{SSM/I}$, but are not sufficient, for air-sea heat flux estimation for studies of climate variations. The monthly-mean fluxes of heat at the ocean surface need to be known to $\pm$ 10 - 15 W m^{-2} for climate variation signals to be recognized [26]. An error of only 0.5 m s^{-1} in wind speed leads to an error of 12 W m^{-2} [28].

The SSM/I provides only wind speed, which limits the usefulness of the data for dynamical ocean circulation studies because the wind velocity vector and its horizontal gradients generate ocean currents. Wind direction must be known. Various schemes are being developed to produce a SSM/I wind speed and direction data product [29, 7]. Had wind direction been determined with wind speed, the accuracy of the RSS wind speed would be improved by about 20% because the 37-GHz brightness temperatures varied by $\pm$ 1 °K depending upon wind direction [7].

ACKNOWLEDGEMENTS

This work would not have been possible without the help of Drs. Stanley Hayes (PMEL), Harunobu Masuko (Communications Research Laboratory, Tokyo), Michael McPhaden (PMEL), Robert Weller (WHOI), and Frank Wentz (RSS), who kindly provided the PMEL (ATLAS array), JMA, PMEL (current-meter array), WHOI, and NDBC moored-buoy wind data, respectively; I am grateful to them. William Knauss (JPL) developed the computer software to track and analyze millions of numbers, all in his usual outstanding fashion. Suggestions by two anonymous reviewers and Dr. James A. Smith, Editor of *TGARS*, were greatly appreciated. This work was supported by NASA UPN 578-22-26-40 and by the NSCAT Project, which are gratefully acknowledged. The research described in this paper was performed by the Jet Propulsion Laboratory, California Institute of Technology, under contract with the National Aeronautics and Space Administration. This paper is dedicated to the memory of Dr. Stanley P. Hayes, who established real-time monitoring of moored-buoy winds in the tropical Pacific.

REFERENCES

[1] Houghton, J.T., G.J. Jenkins and J.J. Ephraums (1990) *Climate Change, The IPCC Scientific Assessment.* Cambridge University Press, New York, 365 pp.

[2] Halpern, D., Zlotnicki, V., Newman, J., Dixon, D., O. Brown and F. Wentz (1992) An atlas of monthly mean distributions of GEOSAT sea surface height, SSM/I surface wind speed, AVHRR/2 sea surface temperature, and ECMWF surface wind components during 1987. JPL Publication 92-3, Jet Propulsion Laboratory, Pasadena, 111 pp.

[3] Wentz, F.J. (1989) User's manual SSM/I geophysical tapes. RSS Technical Report 060989, Remote Sensing Systems, Santa Rosa, California, 16 pp.

[4] Goodberlet, M.A., C.T. Swift and J.C. Wilkerson (1990) Ocean surface wind speed measurements of the Special Sensor Microwave/Imager (SSM/I). *IEEE Transactions on Geoscience and Remote Sensing, 28*, 823-828.

[5] Bates, J.J. (1991) High-frequency variability of Special Sensor Microwave/Imager derived wind speed and moisture during an intraseasonal oscillation. *Journal of Geophysical Research, 96*, 3411-3423.

[6] Schluessel, P. and H. Luthardt (1991) Surface wind speeds over the North Sea from Special Sensor Microwave/Imager Observations. *Journal of Geophysical Research, 96*, 4845-4853.

[7] Wentz, F.J. (1991) Measurement of oceanic wind vector using satellite microwave radiometers. RSS Technical Report 051591, Remote Sensing Systems, Santa Rosa, California, 33 pp.

[8] Halpern, D. (1991) The NASA Ocean Data System at the Jet Propulsion Laboratory. *Advances in Space Research, 11*, 255-262.

[9] Halpern, D., Zlotnicki, V., Newman, J., O. Brown and F. Wentz (1991) An atlas of monthly mean distributions of GEOSAT sea surface height, SSM/I surface wind speed, AVHRR/2 sea surface temperature, and ECMWF surface wind components during 1988. JPL Publication 91-8, Jet Propulsion Laboratory, Pasadena, 110 pp.

[10] Hollinger, J.P., J.L. Pierce and G.A. Poe (1990) SSM/I instrument evaluation. *IEEE*

Transactions on Geoscience and Remote Sensing, *28*, 781-790.

[11] Gilhousen, D.B. (1987) A field evaluation of NDBC moored buoy winds. *Journal of Atmospheric and Oceanic Technology*, *4*, 94-104.

[12] Hayes, S.P., L.J. Mangum, J. Picaut and K. Takeuchi (1991) TOGA-TAO: A moored array for real-time measurements in the tropical Pacific Ocean. *Bulletin of the American Meteorological Society*, *72*, 339-347.

[13] Freitag, H.P., M.J. McPhaden and A.J. Shepherd (1989) Comparison of equatorial winds measured by cup and propeller anemometers. *Journal of Atmospheric and Oceanic Technology*, *6*, 327-332.

[14] Crescenti, G.H., S.A. Tarbell and R.A. Weller (1991) A compilation of moored current meter data and wind recorder data from the Severe Environment Surface Mooring (SESMOOR). Woods Hole Oceanographic Institution Technical Report, WHOI-91-18, Woods Hole Oceanographic Institution, Woods Hole, 49 pp.

[15] Halpern, D. (1987) Comparison of moored wind measurements from a spar and toroidal buoy in the eastern equatorial Pacific during February/March 1981. *Journal of Geophysical Research*, *92*, 8303-8306.

[16] Halpern, D. (1988a) Moored surface wind observations at four sites along the Pacific equator between 140° and 95°W. *Journal of Climate*, *1*, 1251-1260.

[17] Halpern, D. (1979) Surface wind measurements and low-level cloud motion vectors near the Intertropical Convergence Zone in the central Pacific Ocean from November 1977 to March 1978. *Monthly Weather Review*, *107*, 1525-1534.

[18] Hsu, H.-H. and B.J. Hoskins (1989) Tidal fluctuations as seen in ECMWF data. *Quarterly Journal of the Royal Meteorological Society*, *115B*, 247-264.

[19] Halpern, D. (1988b) On the accuracy of monthly mean wind speeds over the equatorial Pacific. *Journal of Atmospheric and Oceanic Technology*, *5*, 362-367.

[20] Trenberth, K.E., W.G. Large and J.G. Olson (1990) The mean annual cycle in global ocean wind stress. *Journal of Physical Oceanography*, *20*, 12742-1760.

[21] Smith, G.M. (1967) *A Simplified Guide to Statistics.* Holt, Rinehart and Winston, New York, 164 pp.

[22] Press, W.H., B.P. Flannery, S.A. Teukolsky and W.T. Vetterling (1988) *Numerical Recipes in C.* Cambridge University Press, New York, 735 pp.

[23] McCreary, J. (1976) Eastern tropical ocean response to changing wind systems: with application to El Niño. *Journal of Physical Oceanography, 6,* 632-645.

[24] Climate Diagnostics Bulletin (1990) Near Real-Time Analyses Ocean-Atmosphere, No. 90/3, edited by V.E. Kousky, Climate Analysis Center, NOAA/NWS/NMC, Washington, 70 pp.

[25] Clayson, C.A. and W.J. Emery (1991) A comparison of SSM/I wind speed algorithms and wind direction calculations. *Eos, Transactions, American Geophysical Union, 72* (51 Supplement), 89.

[26] Bretherton, F. (1981) The ocean surface energetics - a need for climate understanding. In: *Applications of Existing Satellite Data to the Study of the Ocean Surface Energetics,* C. Gautier, editor, University of Wisconsin Press, Madison, 5-14.

[27] Brown, R.A., V.J. Cardone, T. Guymer, J. Hawkins, J. Overland, W.J. Pierson, S. Peteherych, J.C. Wilkerson, P.M. Woiceshyn and M. Wurtele (1982) Surface wind analysis for SEASAT. *Journal of Geophysical Research, 87,* 3355-3364.

[28] Ramage, C.S. (1984) Can shipboard measurements reveal secular changes in tropical air-sea heat flux? *Journal of Climate and Applied Meteorology, 23,* 187-193.

[29] Atlas, R., S.C. Bloom, R.N. Hoffman, J.V. Ardizzone and G. Brin (1991) Space-based surface wind vectors to aid understanding of air-sea interactions. *EOS, Transactions, American Geophysical Union, 72,* 204-206.

LIST OF FIGURES

deviations of average $|S_{SSM/I} - S_{BUOY}|$ computed within the 0.25 m s^{-1} interval of the monthly distribution of $S_{SSM/I}$. Smallest number of values to calculate the average $|S_{SSM/I} - S_{BUOY}|$ value was 17; maximum was 91.

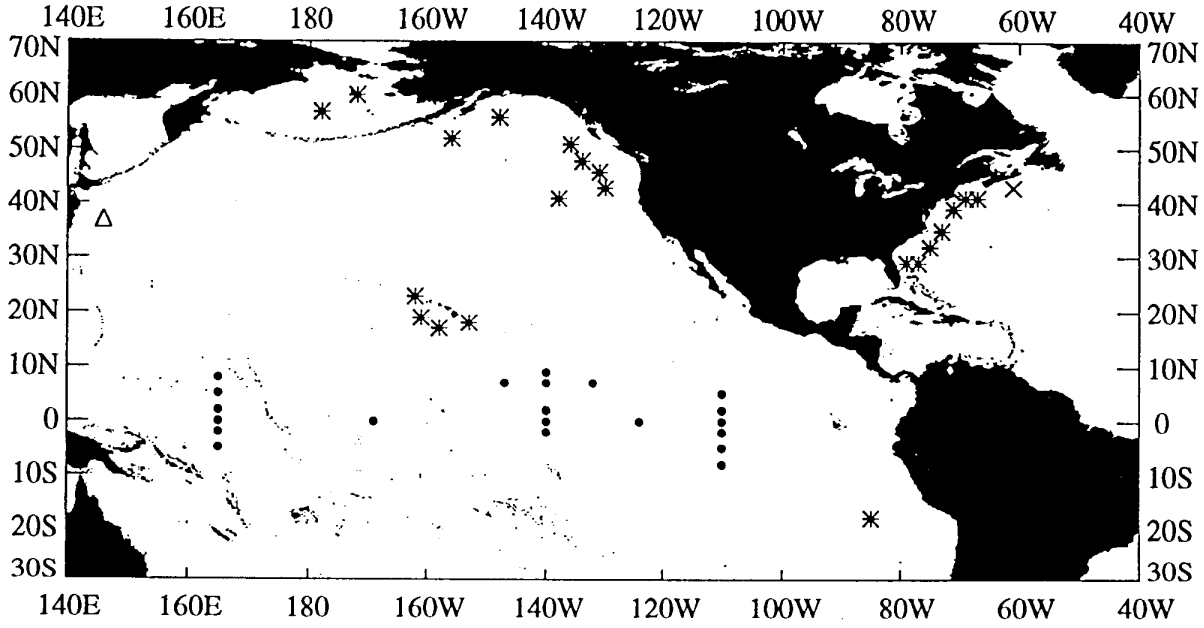
140E
160E
180
160W
140W
120W
100W
80W
60W
40W
70N
60N
50N
40N
30N
20N
10N
0
10S
20S
30S

Figure 1

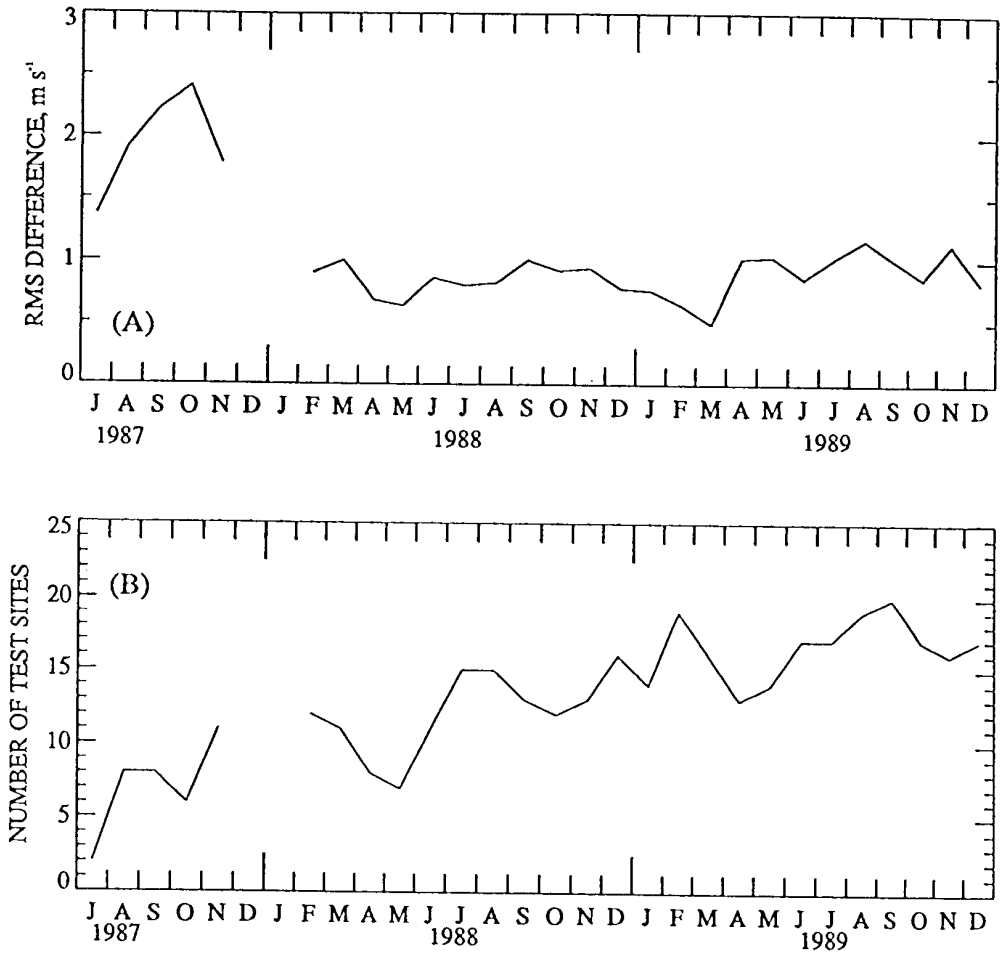
RMS DIFFERENCE, m s⁻¹
3
2
1
0
(A)
J A S O N D J F M A M J J A S O N D J F M A M J J A S O N D
1987
1988
1989
NUMBER OF TEST SITES
25
20
15
10
5
0
(B)
J A S O N D J F M A M J J A S O N D J F M A M J J A S O N D
1987
1988
1989

Figure 2

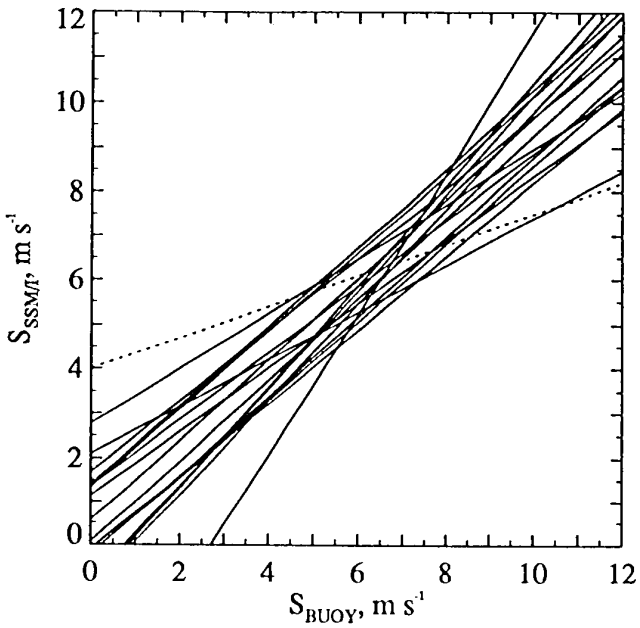

Figure 3

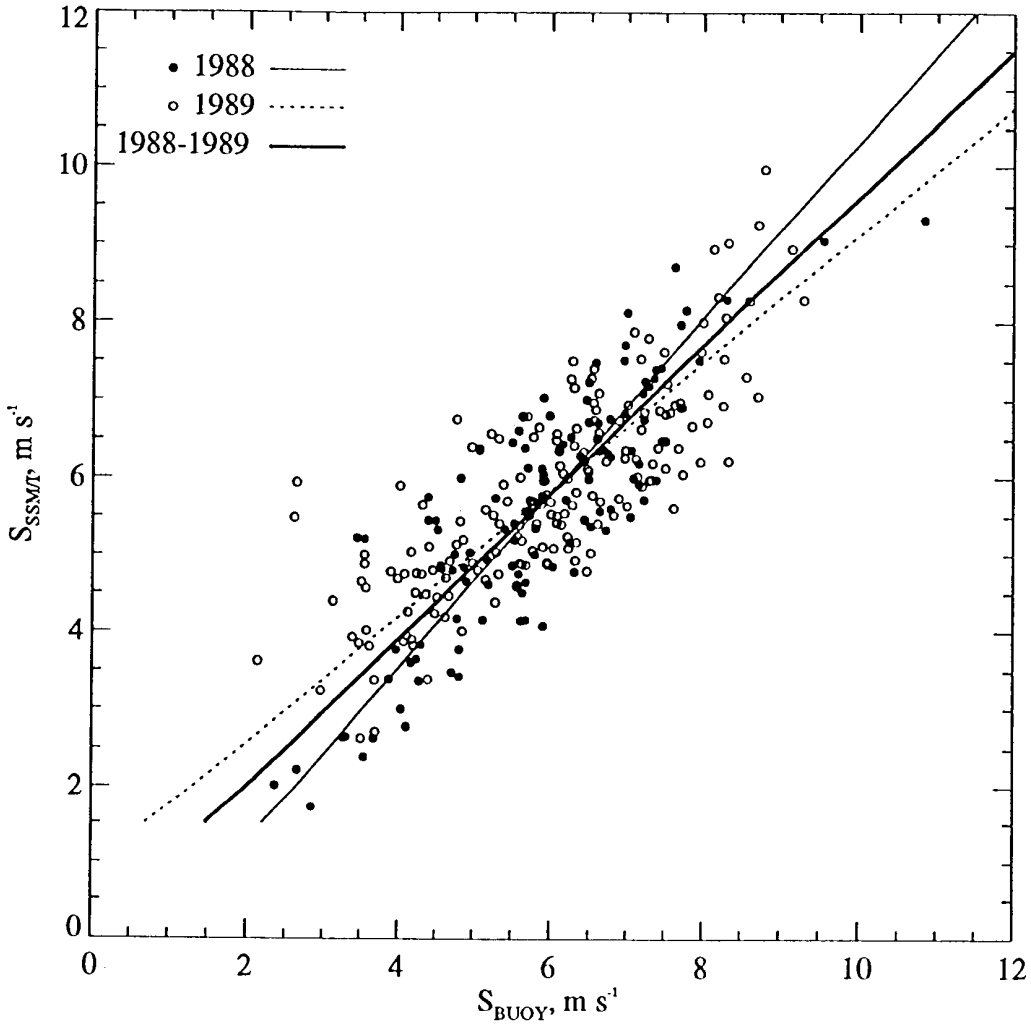

Figure 4

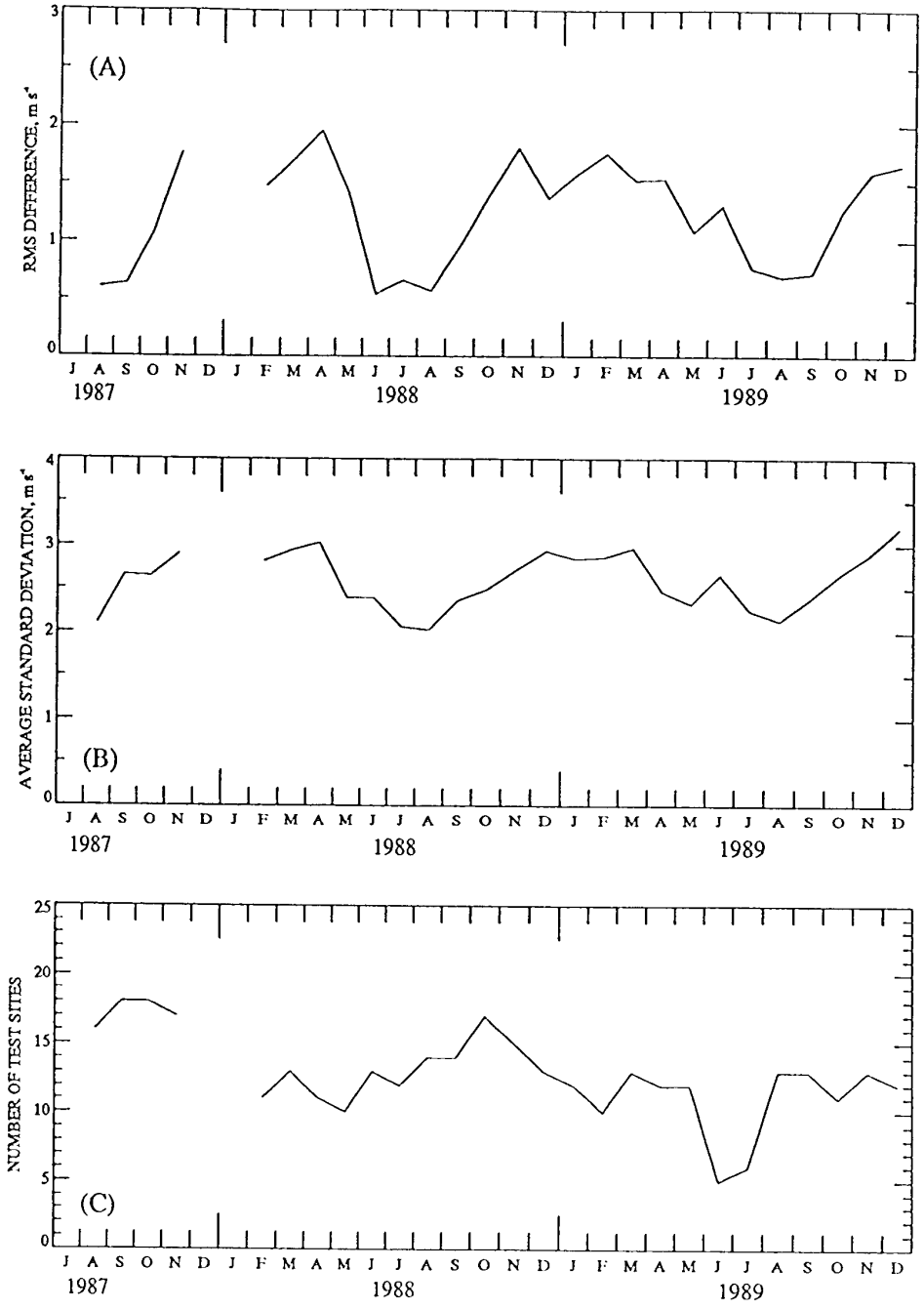
(A)
RMS DIFFERENCE, m s⁻¹
3
2
1
0
J A S O N D J F M A M J J A S O N D J F M A M J J A S O N D
1987
1988
1989
(B)
AVERAGE STANDARD DEVIATION, m s⁻¹
4
3
2
1
0
J A S O N D J F M A M J J A S O N D J F M A M J J A S O N D
1987
1988
1989
(C)
NUMBER OF TEST SITES
25
20
15
10
5
0
J A S O N D J F M A M J J A S O N D J F M A M J J A S O N D
1987
1988
1989

Figure 5

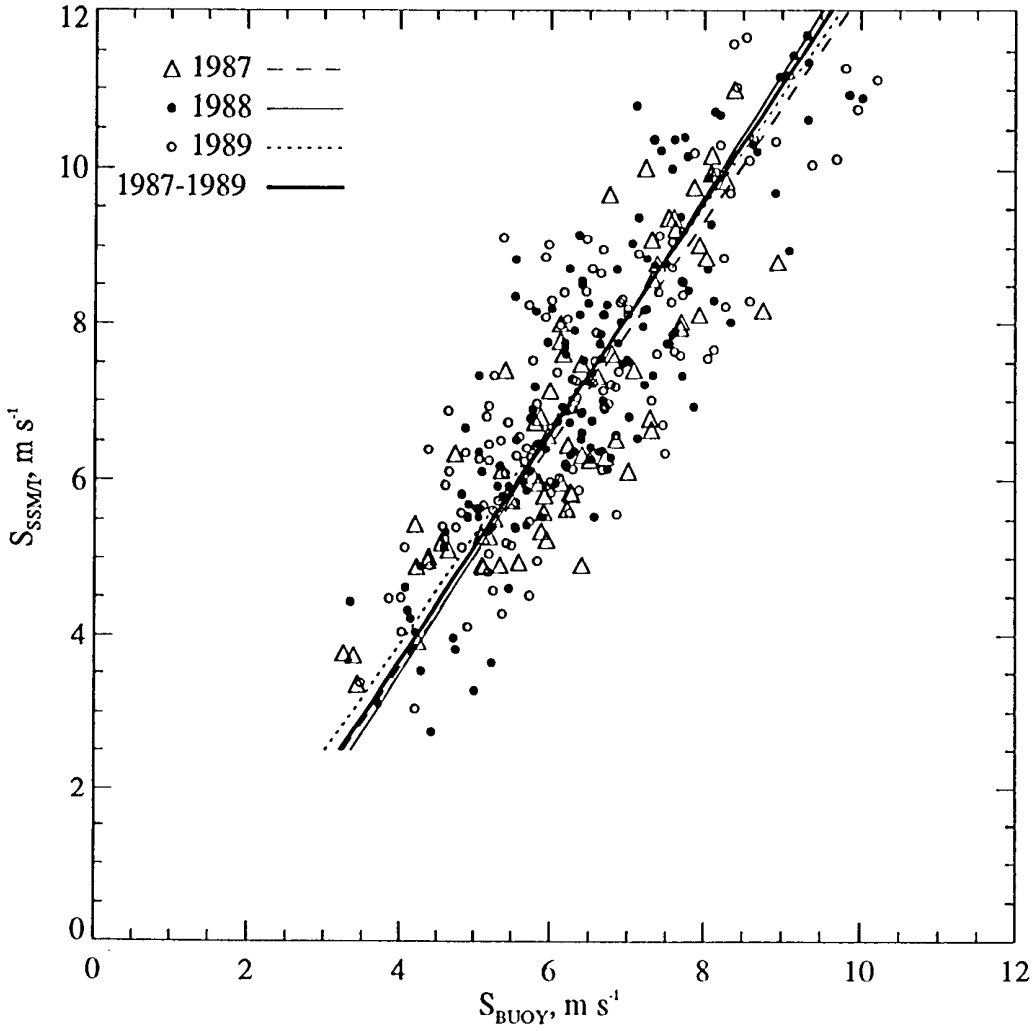

Figure 6

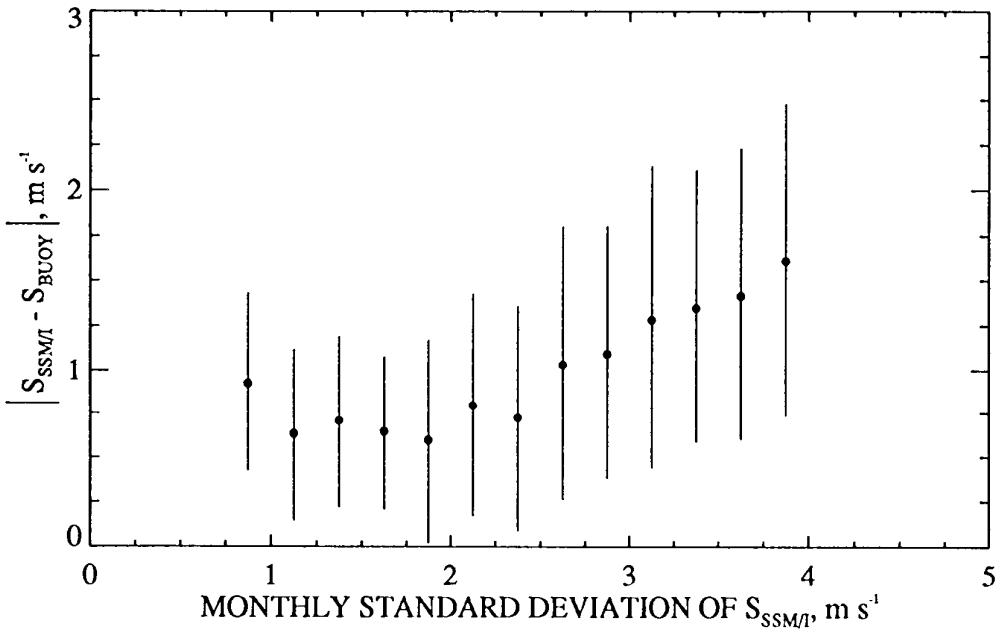
3
2
1
0
0
1
2
3
4
5
$|S_{SSM/I} - S_{BUOY}|$, m s^{-1}
MONTHLY STANDARD DEVIATION OF $S_{SSM/I}$, m s^{-1}

Figure 7